Received: 16 May 2022 | Revised: 25 August 2022 | Accepted: 18 September 2022

DOI: 10.1049/cth2.12363

IET Control Theory & Applications

The Institution of Engineering and Technology WILEY

ORIGINAL RESEARCH

Deterministic submanifolds for the backward-evolving quantum state concerning a monitored qubit

Zibo Miao[1] | **Zigui Zhang**[1] | **Kai Li**[1] | **Yu Pan**[2] | **Alain Sarlette**[3,4]

[1]School of Mechanical Engineering and Automation, Harbin Institute of Technology, Shenzhen, China

[2]State Key Laboratory of Industrial Control Technology, Institute of Cyber-Systems and Control, College of Control Science and Engineering, Zhejiang University, Hangzhou, China

[3]LPENS, Physics Department, Ecole Normale Supérieure, Centre Automatique et Systémes (CAS), MINES ParisTech, Université PSL, Sorbonne Université, CNRS, Inria, Paris, France

[4]Department of Electronics and Information Systems, Ghent University, Beligum

Correspondence
Zibo Miao, School of Mechanical Engineering and Automation, Harbin Institute of Technology, Shenzhen 518055, China.
Email: miaozibo@hit.edu.cn

Funding information
Agence Nationale de la Recherche, Grant/Award Number: HAMROQS; National Natural Science Foundation of China, Grant/Award Numbers: 62003113, 62173296

Abstract

The evolution of a quantum system subject to continuous weak measurement is described by a stochastic differential equation (SDE). It has been shown that the conventional density matrix ρ_t characterized by such SDE, under experimentally relevant settings, remains within a deterministically evolving manifold of low dimension, whose associated equations can be computed explicitly. In this paper, as a complement, it is demonstrated that the effect matrix E_t, associated to a quantum system at the time t to express its measurement during the interval $[t, T]$, also remains confined to a deterministically evolving manifold. In particular, by using the Bloch sphere representation together with the properties of Pauli matrices (as the quantum representation of quaternions), deterministic submanifolds for the effect matrix concerning a monitored qubit are given explicitly. The qubit stays on a deterministically evolving curve in the homodyne amplitude detection scenario, and on a deterministically moving surface under heterodyne amplitude detection. This deterministic characterization should be of interest for parameter estimation and towards obtaining computationally efficient quantum filters for real-time quantum control.

1 | INTRODUCTION

Quantum stochastic differential equations provide a generic framework to describe the dynamics of an open quantum system. When the system is continuously monitored with the measurement outcome recorded, quantum conditional expectation of the quantum stochastic differential equation gives a quantum stochastic master equation, which plays the role of a continuous-time mathematical model for Markovian evolution [1]. In particular, for a target quantum system defined on a Hilbert space $\mathcal{H}$, in the presence of continuous weak measurement of an output signal amplitude, the conventional quantum state described by the density operator ρ_t evolves according to the following stochastic master equation in the Ito sense:

$$d\rho_t = -\mathrm{i}[H, \rho_t]dt + \sum_{k=1}^{m} F^f_{L_k}(\rho_t)dt + \sum_{k=1}^{m} G^f_{L_k}(\rho_t)\sqrt{\eta_k}dW_t^k, \tag{1}$$

$$dY_t^k = \sqrt{\eta_k}\mathrm{tr}\left(L_k\rho_t + \rho_t L_k^\dagger\right)dt + dW_t^k.$$

Here H and L_k denote the Hamiltonian and output coupling operators, respectively; Y_t^k is the k-th component of the output signal, whose stochastic nature is expressed by an independent Wiener noise process W_t^k and whose informational efficiency (hence, the strength of its backaction on state estimate) is expressed by $\eta_k \geq 0$. The super-operators $F^f_L(\cdot)$ and $G^f_L(\cdot)$ are given by (the superscript ^{f} represents "forward")

$$F^f_L(\rho) = L\rho L^\dagger - \frac{1}{2}L^\dagger L\rho - \frac{1}{2}\rho L^\dagger L,$$

$$G^f_L(\rho) = L\rho + \rho L^\dagger - \mathrm{tr}\left(L\rho + \rho L^\dagger\right)\rho. \tag{2}$$

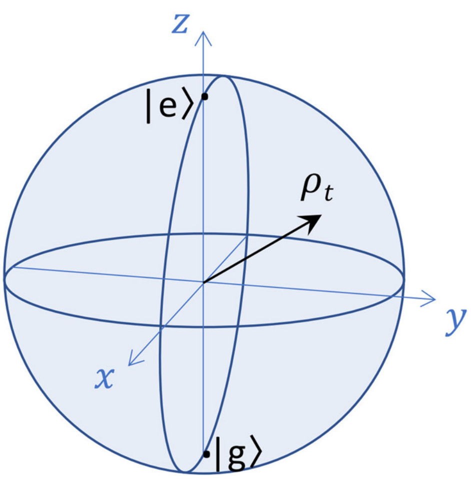

FIGURE 1 The Bloch sphere representation of a qubit

In [2], deterministic submanifolds and analytic solution of the quantum stochastic master equation describing a monitored qubit (related to the conventional density matrix ρ_t) have been provided. On the other hand, as discussed in [3], when ρ_t (depending on the measurement signal before the current time t) combines with the effect matrix E_t (depending on the measurement signal after the current time t and also sometimes called "backward-evolving quantum state"), measurements of limited efficiency can be better interpreted than with ρ_t alone. This is in alignment with quantum state smoothing[4], and leads to further relevant studies in [5–9].

Mainly inspired by the work [2] and [3], in this paper we focus on the backward-evolving quantum state concerning a monitored qubit. The qubit is the smallest quantum system, with two-dimensional Hilbert space $\mathcal{H} = \mathbb{C}^2$. It is the basic unit in quantum computation and communication, and thus sees fruitful applications in various quantum technologies [1, 10–13]. The quantum state of a qubit can be described by a Bloch vector (see Figure 1), associated with Pauli operators.

The Pauli operators are in fact in one-to-one correspondence with the quaternion basis [14–17], complemented by the identity operator for the quaternion real part. Indeed, they both generate a faithful representation of the special unitary group $SU(2)$, while the wavefunction of a quantum system on $\mathcal{H} = \mathbb{C}^n$ is exactly described by an evolution in $SU(n)$. In matrix form, the Pauli operators $\{\sigma_x, \sigma_y, \sigma_z\}$ can be represented as follows:

$$\sigma_x = \begin{bmatrix} 0 & 1 \\ 1 & 0 \end{bmatrix}, \sigma_y = \begin{bmatrix} 0 & -\mathrm{i} \\ \mathrm{i} & 0 \end{bmatrix}, \sigma_z = \begin{bmatrix} 1 & 0 \\ 0 & -1 \end{bmatrix}, \tag{3}$$

where i denotes the imaginary unit. The action of the σ_x operator is said to introduce a "bit flip", the action of the σ_z operator is to introduce a "phase flip", and the action of the σ_y operator is to introduce simultaneously the bit and phase flips. A representation of $SU(2)$ is obtained by taking the exponential of any real linear combination of imaginary unit times the Pauli operators. Accordingly, these operators satisfy properties analogous to the quaternion basis elements i, j, k:

$$\begin{aligned} & i^2 = j^2 = k^2 = -1 \\ \leftrightarrow\ & (\mathrm{i}\sigma_y)^2 = (\mathrm{i}\sigma_x)^2 = (\mathrm{i}\sigma_z)^2 = -I, \\ & ij = k,\ jk = i,\ ki = j \\ \leftrightarrow\ & (\mathrm{i}\sigma_y)(\mathrm{i}\sigma_x) = \mathrm{i}\sigma_z,\ (\mathrm{i}\sigma_x)(\mathrm{i}\sigma_z) = \mathrm{i}\sigma_y,\ (\mathrm{i}\sigma_z)(\mathrm{i}\sigma_y) = \mathrm{i}\sigma_x. \end{aligned} \tag{4}$$

By using the Bloch sphere representation together with the properties of Pauli matrices, we show in Section 3 how the *normalized version* ξ_t of the backward-evolving state E_t of a monitored qubit stays on a deterministically evolving submanifold much like its forward-evolving counterpart ρ_t, in similar measurement scenarios. In Section 2, we develop the evolution for the normalized effect matrix ξ_t. Section 4 provides some concluding remarks and future research directions.

2 | NORMALIZED EFFECT MATRIX ξ_t FOR THE BACKWARD-EVOLVING QUANTUM STATE

In order to obtain the deterministic submanifolds for the backward-evolving quantum state concerning a monitored qubit, we first develop the equation of motion for normalized effect matrix ξ_t (note that the backward evolving effect matrix E_t in [3], associated to a quantum system at the time t to express its measurement during the interval $[t, T]$, is not normalized). According to [3], the not-trace-preserving evolution equation for E_t is given by

$$\begin{aligned} dE_t = {} & \mathrm{i}[H, E_t]dt + \sum_{k=1}^{m} \sqrt{\eta_k}\left(L_k^\dagger E_t + E_t L_k\right) dY_{t-dt}^k \\ & + \sum_{k=1}^{m}\left(L_k^\dagger E_t L_k - \frac{1}{2}\left\{L_k^\dagger L_k, E_t\right\}\right)dt, \end{aligned} \tag{5}$$

with the final effect matrix being E_T (e.g. $E_T = I$). Note that here dt is positive and $dE_t = E_{t-dt} - E_t$, propagating backward from T to t using the measurement record dY_t^k determined by

$$dY_t^k = \sqrt{\eta_k}\mathrm{tr}\left(L_k\rho_t + \rho_t L_k^\dagger\right)dt + dW_t^k. \tag{6}$$

The normalization of E_t is denoted by $\xi_t = \frac{E_t}{\mathrm{tr}(E_t)}$, with the final condition $\xi_T = \frac{E_T}{\mathrm{tr}(E_T)}$, and one can derive that the normalized effect matrix evolves as follows:

$$\begin{aligned} d\xi_t = {} & \mathrm{i}[H, \xi_t]dt + \sum_{k=1}^{m} F_{L_k}^b(\xi_t)dt \\ & + \sum_{k=1}^{m} G_{L_k}^b(\xi_t)\sqrt{\eta_k}dW_{t-dt}^k, \end{aligned} \tag{7}$$

where $F_L^b(\xi_t) : \mathcal{H} \mapsto \mathcal{H}$ and $G_L^b(\xi_t) : \mathcal{H} \mapsto \mathcal{H}$ are defined as (the superscript ^{b} represents "backward")

$$\begin{aligned} F_L^b(\xi_t) &= L^\dagger \xi_t L - \frac{1}{2}\left\{L^\dagger L, \xi_t\right\} - \mathrm{tr}\left(LL^\dagger \xi_t - L^\dagger L \xi_t\right)\xi_t \\ &+ \eta\left(L^\dagger \xi_t + \xi_t L - \mathrm{tr}\left(L^\dagger \xi_t + \xi_t L\right)\xi_t\right)\mathrm{tr}\left(L\rho_{t-dt} + \rho_{t-dt}L^\dagger\right) \\ &- \eta\left(L^\dagger \xi_t + \xi_t L - \mathrm{tr}\left(L^\dagger \xi_t + \xi_t L\right)\xi_t\right)\mathrm{tr}\left(L^\dagger \xi_t + \xi_t L\right), \end{aligned} \tag{8}$$

and

$$G_L^b(\xi_t) = L^\dagger \xi_t + \xi_t L - \mathrm{tr}\big(L^\dagger \xi_t + \xi_t L\big)\xi_t, \tag{9}$$

respectively. It can be verified that $d(\xi_t \mathrm{tr}(E_t)) = dE_t$ during the time interval $[t, T]$ according to equations (7)–(9).

This SDE must still be understood in the Ito sense and is nonlinear. It involves vector fields of random amplitude, owing to the stochastic measurement results, of directions $G_{L_k}^b$. Note that this involves both direct contribution of the second line in (7), as well as indirect contribution through the second line of (8). Indeed, the latter involves past (random) values of dW_t through ρ_{t-dt}. We will treat all these contributions as vector fields which can push ξ_t around in state space with unknown amplitudes. When these vector fields, evaluated at any ξ_t, do not span all the directions of state space, there may exist sub-manifolds to which the state ξ_t remains confined irrespectively of the measurement results. The $G_{L_k}^b$ must all be tangent to such sub-manifold, and for the manifold to actually persist it must "commute with" the deterministic part of the vector field. As explained in [2], after an Ito-to-Stratonovich transformation of the SDE, the existence of such confinement can hence be studied much like in classical controllability results, while the directions $G_{L_k}^b$ give hints on how to explicitly compute the equations of the time-dependent nonlinear sub-manifold.

While [2] applies this program to the evolution of the forward-evolving state ρ_t of a qubit, we here establish similar properties for the normaliser backward-evolving state ξ_t.

3 | DETERMINISTIC SUBMANIFOLDS FOR ξ_t CONCERNING A MONITORED QUBIT

In this section, we will consider two measurement scenarios of a monitored qubit. That is, the homodyne measurement and heterodyne measurement, both with $H = 0$. In homodyne detection [Ho], the dynamic equation involves a single monitored channel L_1 while in heterodyne detection [He] it features two channels L_1 and $L_2 = iL_1$, with the same measurement efficiency $\eta_1 = \eta_2 = \eta$. In terms of the L_1 operator, we consider two schemes. In one of the schemes, we take L_1 a Hermitian operator [H], denoted by $L_1 = \sigma_z = |e\rangle\langle e| - |g\rangle\langle g|$, which physically corresponds to a quantum non-demolition (QND) measurement. In the other scheme, L_1 is chosen to be $L_1 = \sigma_- = |g\rangle\langle e| = (\sigma_x - i\sigma_y)/2$, which is nilpotent [N] and physically corresponds to a fluorescence measurement. Like the conventional qubit density matrix ρ_t, the normalized ξ_t can be characterized by a Bloch vector whose components x_e, y_e and z_e express the state in the Pauli operators basis. These coordinates represent the actual Cartesian coordinates in the Bloch sphere of Figure 1.

Denote $\xi_t = \frac{I + x_e(t)\sigma_x + y_e(t)\sigma_y + z_e(t)\sigma_z}{2}$ and $\rho_t = \frac{I + x_\rho(t)\sigma_x + y_\rho(t)\sigma_y + z_\rho(t)\sigma_z}{2}$. We take the scenario heterodyne measurement with $L_1 = \sigma_-$ and $L_2 = i\sigma_-$ [HeN] as a calculation example. By plugging the above form of $\xi_t(\rho_t)$ in equation (7), working out the operators using Pauli operator properties (4) and identifying the components of $\sigma_x, \sigma_y, \sigma_z$ on both sides of the equation, one obtains that

$$\begin{aligned} dx_e &= x_e(2z_e - 1)dt + \eta(1 - z_e - x_e^2)(x_\rho - x_e)dt \\ &\quad - \eta x_e y_e (y_\rho - y_e)dt \\ &\quad + \sqrt{\eta}(1 - z_e - x_e^2)dW_1 - \sqrt{\eta} x_e y_e dW_2, \end{aligned} \tag{10}$$

$$\begin{aligned} dy_e &= y_e(2z_e - 1)dt - \eta x_e y_e (x_\rho - x_e)dt \\ &\quad + \eta(1 - z_e - y_e^2)(y_\rho - y_e)dt \\ &\quad - \sqrt{\eta} x_e y_e dW_1 + \sqrt{\eta}(1 - z_e - y_e^2)dW_2, \end{aligned} \tag{11}$$

$$\begin{aligned} dz_e &= 2(-z_e + z_e^2)dt + \eta(x_e - x_e z_e)(x_\rho - x_e)dt \\ &\quad + \eta(y_e - y_e z_e)(y_\rho - y_e)dt \\ &\quad + \sqrt{\eta}(x_e - x_e z_e)dW_1 + \sqrt{\eta}(y_e - y_e z_e)dW_2, \end{aligned} \tag{12}$$

where $x_e = x_e(t)$, $y_e = y_e(t)$, and $z_e = z_e(t)$; $x_\rho = x_\rho(t - dt)$, $y_\rho = y_\rho(t - dt)$, and $z_\rho = z_\rho(t - dt)$; $dW_1 = dW_1(t - dt)$ and $dW_2 = dW_2(t - dt)$.

Transforming this to cylindrical coordinates (r_e, θ_e and z_e), while taking care to use the appropriate rules of Ito calculus, we have that

$$\begin{aligned} dr_e &= r_e\big(2z_e - 1\big)dt + \frac{\eta\big(1 - z_e\big)^2}{2r_e}dt \\ &\quad + \eta\big(1 - z_e - r_e^2\big)\big(x_\rho \cos\theta + y_\rho \sin\theta - r_e\big)dt \\ &\quad + \sqrt{\eta}\big(1 - z_e - r_e^2\big)(\cos\theta dW_1 + \sin\theta dW_2), \end{aligned} \tag{13a}$$

$$\begin{aligned} dz_e &= 2\big(z_e^2 - z_e\big)dt \\ &\quad + \eta r_e\big(1 - z_e\big)\big(x_\rho \cos\theta + y_\rho \sin\theta - r_e\big)dt \\ &\quad + \sqrt{\eta} r_e\big(1 - z_e\big)(\cos\theta dW_1 + \sin\theta dW_2), \end{aligned} \tag{13b}$$

$$\begin{aligned} d\theta_e &= \eta\frac{1 - z_e}{r_e}\big(-x_\rho \sin\theta + y_\rho \cos\theta\big)dt \\ &\quad + \sqrt{\eta}\frac{1 - z_e}{r_e}(-\sin\theta dW_1 + \cos\theta dW_2). \end{aligned} \tag{13c}$$

Equations like (13) contain two random signals W_1 and W_2 for a three-dimensional state space. For homodyne detection, we even have a single random signal W_1 for the three-dimensional state space. In general, a single scalar control signal in combination with a fixed drift vector field would enable us to explore the full state space (see standard controllability analysis). However, remarkably, it has been observed in actual experiments that for this particular dynamics, different signals $W_1(t)$ and $W_2(t)$ do not diffuse the state ρ_t in all directions; instead, ρ_t is maintained within a specific time-dependent ellipsoid, for various initial states and independently of the output signals [2, 18]. Inspired by these results, we postulate a similar behavior for ξ_t. We hence consider candidate confinement surfaces defined by

$$\frac{r_e^2}{2} + f_c(z_e) = 0 \tag{14}$$

where f_c is a function to be found, and $c \in \mathbb{R}$ parametrizes how the surface evolves over time. Since the purely stochastic part of the motion is supposed to be tangent to this surface, one has to require that

$$r_e\left(1 - z_e - r_e^2\right) + \frac{df_c}{dz_e} r_e(1 - z_e) = 0. \tag{15}$$

This then leads to the following theorem for the heterodyne detection case (in the presence of two random signals):

Theorem 1.

(a) *The normalized backward state ξ_t for a monitored qubit in the [HeH] scenario remains at all times confined to the surface defined by*

$$r_e^2 - b_t\,(1 - z_e^2) = 0, \tag{16}$$

where $b_t = b_T e^{8(1-\eta)(T-t)}$, $t \in [0, T]$.

(b) *The normalized backward state ξ_t for a monitored qubit in the [HeN] scenario remains at all times confined to the surface defined by*

$$\frac{r_e^2}{2} + c_t(1 - z_e)^2 - (1 - z_e) = 0\ , \tag{17}$$

where $c_t = (1 - \frac{\eta}{2}) + e^{2(T-t)}(c_T - (1 - \frac{\eta}{2}))$, $t \in [0, T]$.

Proof. In the [HeN] scenario, according to the analysis above, since

$$r_e\left(1 - z_e - r_e^2\right) + \frac{df_c}{dz_e} r_e(1 - z_e) = 0, \tag{18}$$

we can further have that

$$f_c = c_t(1 - z_e)^2 - (1 - z_e), \tag{19}$$

with

$$dc_t = 2\left(1 - \frac{\eta}{2} - c_t\right) dt. \tag{20}$$

We then are able to obtain the deterministic surface in the backward evolving manner as specified in Theorem 1(b).

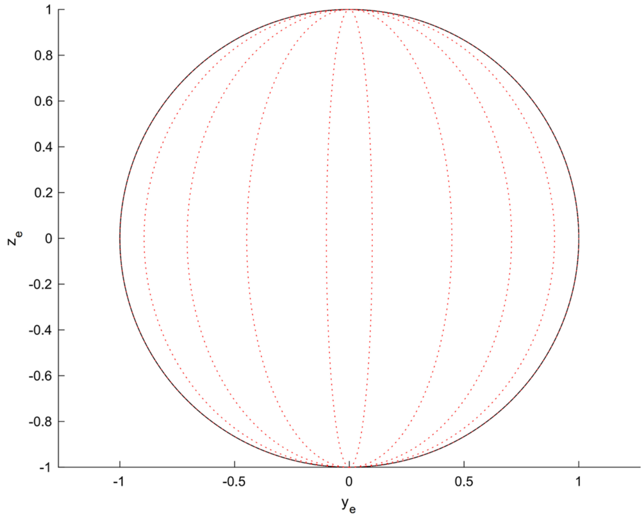

FIGURE 2 [HeH] scenario: plot of curves resulting from the intersection of the plane $x_e = 0$ with the surface described by $r_e^2 - b_t\,(1 - z_e^2) = 0$, for $b_t \in \{1, 0.8, 0.5, 0.2, 0.01\}$, respectively, from outer to inner ellipse

In the [HeH] scenario, the evolution for ξ_t in cylindrical coordinates can be given by

$$dr_e = r_e(2\eta - 4)dt + 4\eta r_e z_e(z_e - z_\rho)dt - 2\sqrt{\eta}\, r_e z_e dW_1, \tag{21a}$$

$$dz_e = 4\eta(z_e^2 - 1)(z_e - z_\rho)dt + 2\sqrt{\eta}(1 - z_e^2)dW_1, \tag{21b}$$

$$d\theta_e = 2\sqrt{\eta}\, dW_2. \tag{21c}$$

By following the same principles as shown in the [HeN] scenario to calculate the deterministic surface, one can obtain equation (16) in Theorem 1(a). □

The two situations are depicted on Figures 2 and 3, respectively. For the scenario [HeH], the ellipsoids go from the unit sphere for $b_t = 1$ to the polar axis for $b_t = 0$. The initialization $\xi_T = \frac{I}{2}$ when $E_T = I$, with $r_e(T) = z_e(T) = 0$, corresponds to $b_T = 0$. Therefore, with such initialization, the normalized backward state ξ_t remains at the polar axis. In particular, for a unit efficiency $\eta = 1$, thus $b_t = b_T$, the state always stays on the initialized ellipsoid; otherwise, as t decreases, the value of b_t increases and hence the ellipse grows exponentially. For the scenario [HeN], the surface coincides with the unit sphere when $c_t = 0.5$, and as c_t increases, it flattens and shrinks towards the point $z_e = 1$, corresponding to $\xi_t = |e\rangle\langle e|$. For example, the initialization $r_e(T) = \frac{\sqrt{3}}{2}$, $z_e(T) = \frac{1}{2}$, corresponds to $c_T = 0.5$. From there, as t decreases from T to 0, the value of c_t exponentially increases and hence the ellipse shrinks.

For homodyne detection, a single measurement channel and hence a single stochastic signal is present. One computes that, like for ρ_t as shown in [2], in both qubit settings considered the state ξ_t remains confined to a deterministic curve irrespectively of the measurement results. For instance, for the homodyne

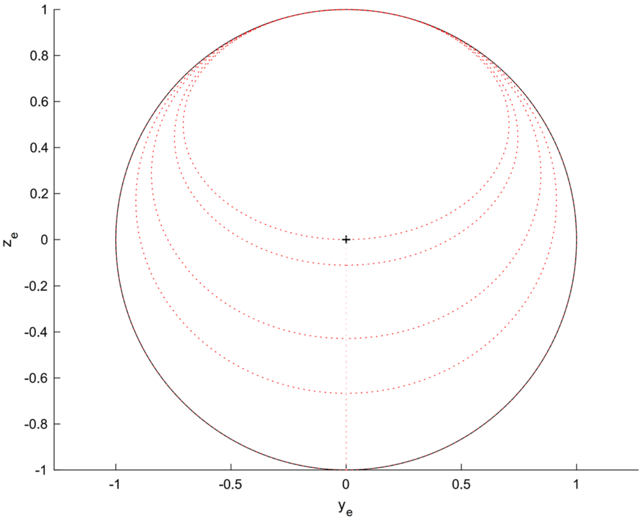

FIGURE 3 [HeN] scenario: plot of curves resulting from the intersection of the plane $x_e = 0$ with the surface described by $\frac{r_e^2}{2} + c_t(1-z_e)^2 - (1-z_e) = 0$, for $c_t \in \{0.5, 0.6, 0.7, 0.9, 1\}$, respectively, from outer to inner ellipse

QND measurement, that is, $L_1 = \sigma_z$, we obtain the evolution for ξ_t given by

$$dx_e = -\left(2 + 4\eta z_\rho z_e - 4\eta z_e^2\right) x_e dt - 2\sqrt{\eta} z_e x_e dW_1, \tag{22}$$

$$dy_e = -\left(2 + 4\eta z_\rho z_e - 4\eta z_e^2\right) y_e dt - 2\sqrt{\eta} z_e y_e dW_1, \tag{23}$$

$$dz_e = 4\eta(1 - z_e^2)(z_\rho - z_e)dt + 2\sqrt{\eta}(1 - z_e^2)dW_1. \tag{24}$$

In cylindrical coordinates, this gives the following equations:

$$dr_e = -\left(2 + 4\eta z_\rho z_e - 4\eta z_e^2\right) r_e dt - 2\sqrt{\eta} z_e r_e dW_1, \tag{25a}$$

$$dz_e = 4\eta \left(1 - z_e^2\right)(z_\rho - z_e)dt + 2\sqrt{\eta}\left(1 - z_e^2\right) dW_1, \tag{25b}$$

$$d\theta_e = 0. \tag{25c}$$

For the homodyne fluorescence measurement with $L_1 = \sigma_-$, the evolution for ξ_t can be given by

$$dx_e = \eta\left(1 - z_e - x_e^2\right)(x_\rho - x_e)dt + x_e\left(z_e - \frac{1}{2}\right)dt$$
$$+ \sqrt{\eta}\left(1 - z_e - x_e^2\right) dW_1, \tag{26a}$$

$$dy = \eta x_e y_e (x_e - x_\rho)dt + y_e\left(z_e - \frac{1}{2}\right)dt - \sqrt{\eta} x_e y_e dW_1, \tag{26b}$$

$$dz_e = \left(z_e^2 - z_e\right)dt + \eta x_e(1 - z_e)(x_\rho - x_e)dt$$
$$+ \sqrt{\eta} x_e (1 - z_e) dW_1. \tag{26c}$$

Remarkably, despite the presence of z_ρ and x_ρ in these equations, one can obtain the following theorem by means of similar techniques to the heterodyne measurement scenario:

Theorem 2.

(a) The normalized backward state ξ_t for a monitored qubit in the [HoH] scenario remains at all times confined to the curve defined by

$$\theta_t = \theta_T \text{ and } r_e^2 - b_t(1 - z_e^2) = 0, \tag{27}$$

where $b_t = b_T e^{4(1-\eta)(T-t)}$, $t \in [0, T]$.

(b) The normalized backward state ξ_t for a monitored qubit in the [HoN] scenario remains at all times confined to the curve defined by

$$\frac{x_e^2}{2} + c_t(1 - z_e)^2 - (1 - z_e) = 0 \text{ and}$$
$$y_e - d_t(1 - z_e) = 0, \tag{28}$$

where $c_t = 1 - \frac{\eta}{2} + e^{T-t}(c_T - (1 - \frac{\eta}{2}))$ and $d_t = d_T e^{\frac{T-t}{2}}$, $t \in [0, T]$.

The proof of Theorem 2 is analogous to that of Theorem 1, and thus the details are omitted here. In fact, the statements can be verified by showing that the variables b_t, c_t and d_t, *defined* by (17), (16), (27) or (28), respectively, indeed obey the stated autonomous differential equations without being influenced by the noise processes.

4 | CONCLUSIONS AND FUTURE WORK

In this paper we develop deterministically evolving nonlinear submanifolds to which the normalized backward quantum state ξ_t of a monitored qubit is confined independently of the measurement results. This is a remarkable and practically relevant example of a system whose stochastic component does not induce diffusion over the whole state space, allowing for an a priori reduction of the system model. Combined with previous results regarding the conventional forward quantum state ρ_t, better estimation or more computationally efficient quantum filters could be obtained. For instance, the reduction to one or two stochastic variables could make it possible, like in previous work by expanding the probability distribution on the Fourier basis functions to obtain the Fokker–Planck equation in convenient coordinates [2], to explicitly compute the probability distribution over the deterministic submanifold (predicted measurement results). It thus simplifies the control of such systems in the presence of more a priori information. While the case of the qubit, akin to quaternions, is a good pedagogical example, future work will also take into account the possibilities of more powerful model reduction, for higher-dimensional systems.

AUTHOR CONTRIBUTIONS

Zibo Miao: Conceptualization, formal analysis, funding acquisition, methodology, supervision, writing - original draft. Zigui Zhang: Formal analysis, investigation, writing - review and editing. Kai Li: Visualization, writing - original draft, writing - review and editing. Yu Pan: Formal analysis, writing - original draft,

writing - review and editing. Alain Sarlette: Conceptualization, formal analysis, methodology, writing - review and editing.

ACKNOWLEDGEMENTS

The authors acknowledge support by National Natural Science Foundation of China under Grant Nos. 62003113 and 62173296 and by the ANR project grant HAMROQS (French National Research Agency).

CONFLICT OF INTEREST

The authors have declared no conflict of interest.

DATA AVAILABILITY STATEMENT

Data sharing not applicable to this article as no datasets were generated or analysed during the current study.

ORCID

Zibo Miao https://orcid.org/0000-0001-9766-7837

REFERENCES

1. Nielsen, M.A., Chuang, I.L.: Quantum Computation and Quantum Information, 10th anniversary ed. Cambridge University Press, Cambridge (2010)
2. Sarlette, A., Rouchon, P.: Deterministic submanifolds and analytic solution of the stochastic differential master equation describing a qubit. J. Math. Phys. 58(6), 062106 (2017)
3. Gammelmark, S., Julsgaard, B., Mølmer, K.: Past quantum states of a monitored system. Phys. Rev. Lett. 111(16), 160401 (2013)
4. Guevara, I., Wiseman, H.: Quantum state smoothing. Phys. Rev. Lett. 115(18), 180407 (2015)
5. Rybarczyk, T., Gerlich, S., Peaudecerf, B., et al.: Forward-backward analysis of the photon-number evolution in a cavity. Phys. Rev. A 91, 062116 (2015)
6. Zhang, J., Mølmer, K.: Prediction and retrodiction with continuously monitored Gaussian state. Phys. Rev. A 96(6), 062131 (2017)
7. Chantasri, A., Guevara, I., Laverick, K.T., Wiseman, H.M.: Unifying theory of quantum state estimation using past and future Information. Phys. Rep. 930, 1–40 (2021)
8. Gao, Q., Zhang, G., Petersen, I.R.: An exponential quantum projection filter for open quantum systems. Automatica 99, 59-68 (2019)
9. Gao, Q., Dong, D., Petersen, I.R., Ding, S.X.: Design of a quantum projection filter. IEEE Trans. Autom. Control 65(8), 3693–3700 (2020)
10. Sayrin, C., Dotsenko, I., Zhou, X., et al.: Real-time quantum feedback prepares and stabilizes photon number states. Nature 477, 73–77 (2011)
11. Miao, Z., Sarlette, A.: Discrete-time reservoir engineering with entangled bath and stabilising squeezed states. Quantum Sci. Technol. 2(3), 034013 (2017)
12. Yoshihara, F., Fuse, T., Ashhab, S., et al.: Superconducting qubit-oscillator circuit beyond the ultrastrong-coupling regime. Nat. Phys. 13, 44–47 (2017)
13. Zanner, M., Orell, T., Schneider, C.M.F., et al.: Coherent control of a multiqubit dark state in waveguide quantum electrodynamics. Nat. Phys. 18, 538–543 (2022)
14. Wu, A.-G., Liu, W., Li, C., Duan, G.-R.: On j-conjugate product of quaternion polynomial matrices. Appl. Math. Comput. 219(24), 11223–11232 (2013)
15. Zhu, Q., Ma, G., Wang, X., Wu, A.-G.: Attitude control without angular velocity measurement for flexible satellites. Chin. J. Aeronaut. 316(6), 1345–1351 (2018)
16. Finkelstein, D., Jauch, J.M., Schiminovich, S., et al.: Foundations of quaternion quantum mechanics. J. Math. Phys. 3(2), 207–220 (1962)
17. Yang, X., Li, C., Song, Q., et al.: Global Mittag-Leffler stability and synchronization analysis of fractional-order quaternion-valued neural networks with linear threshold neurons. Neural Networks 105, 88–103 (2018)
18. Campagne-Ibarcq, P., Six, P., Bretheau, L., et al.: Observing quantum state diffusion by heterodyne detection of fluorescence. Phys. Rev. X 6, 011002 (2016)

How to cite this article: Miao, Z., Zhang, Z., Li, K., Pan, Y., Sarlette, A.: Deterministic submanifolds for the backward-evolving quantum state concerning a monitored qubit. IET Control Theory Appl. 1–6 (2022). https://doi.org/10.1049/cth2.12363